

# Incommensurate Structures in a Two-Subsystem Partially Frustrated Ferrimagnet

S. N. Martynov

*Kirensky Institute of Physics, Siberian Branch, Russian Academy of Sciences, Krasnoyarsk, 660036 Russia*

*e-mail: unonav@iph.krasn.ru*

Received November 1, 2011

A new incommensurate magnetic structure with a locally triangular orientation of spins has been proposed for a two-subsystem magnet with frustrated intersystem exchange and competition between exchanges in one of the subsystems. When the temperature is lowered, this structure appears from the antiferromagnetic state after a first-order phase transition. It transfers to the Yafet–Kittel triangular structure when the threshold conditions for the exchange interactions are fulfilled. An increase in the length of the frustrated exchange bonds leads to the appearance of an incommensurate phase with the local antiferromagnetic orientation of the sublattices in each subsystem between the commensurate antiferromagnetic and Yafet–Kittel phases.

DOI: 10.1134/S0021364012040066

Geometrically frustrated antiferromagnets were intensively studied during the last decades because of a wide variety of unusual magnetic states [1]. The most attention has been paid to magnets with a high degree of degeneracy of the ground state. This degeneracy prevents the formation of long-range magnetic order down to zero temperature [2]. The majority of real frustrated magnets undergo a phase transition with the establishment of long-range order owing to the removal of degeneracy by various mechanisms. These mechanisms include additional magnetic interactions violating the complete frustration over the isotropic exchange such as exchange between distant neighbors [3, 4], dipole–dipole interaction [5], and the Dzyaloshinskii–Moriya interaction [6]. In many cases, the removal of degeneracy is accompanied by the establishment of long-range order with the magnetic structure period incommensurate with the crystallographic one, i.e., an incommensurate magnetic structure. The interaction between two completely degenerate antiferromagnetic sublattices (subsystems) comprising a magnet can also lead to an incommensurate magnetic structure, as was shown in the mean field approximation by Reimers et al. [3] for the  $A_2B_2O_7$  pyrochlore lattice, where A and B are ions of the different magnetic subsystems. In systems with the dominating exchange between ions in nonequivalent positions (intersubsystem exchange), the ground state is a ferrimagnetic collinear structure with the wave vector  $\mathbf{q} = 0$  [3, 7]. An increase in the intrasubsystem antiferromagnetic exchange in one of the subsystems leads to a helical structure with the locally ferrimagnetic orientation of the moments of the different subsystems, as was shown by Kaplan et al. [8, 9] for the  $AB_2O_4$  cubic spinel. The existence of the main unfrustrated

exchange between ions in one magnetic subsystem changes the situation in principle. This problem within the classical homogeneous model was considered for ferrites of mixed composition by Yafet and Kittel [7]. The possible noncollinear phases were determined. The possibility of temperature-induced phase transitions between them was underlined. Another example of a two-subsystem magnet with this exchange ratio can be copper metaborate  $CuB_2O_4$ . Exchange interactions in this compound are performed via boron–oxygen tetrahedra, leading to branched and extended bonds. The paths of three exchange types between ions of the weak subsystem B and ions of the antiferromagnetic sublattices of the subsystem A transform into each other under the rotation around the second-order axes passing through the B ions. This determines the geometrical frustration of these exchanges. Three exchange types exist inside the subsystem B as well, and two of them form zigzag ladder chains along the tetragonal axis [10]. This combination of exchange bonds leads to the variety of the temperature- and field-induced phase transitions [11]. The form of the low-temperature incommensurate phase in this compound has not yet been determined. In systems with the dominating unfrustrated antiferromagnetic interaction in one of the subsystems ( $J_a$ ), when the temperature decreases, the antiferromagnetic ordering of the moments of this subsystem (A) first takes place. If the intersubsystem exchange  $J_{ab}$  is geometrically frustrated, the spins of the second (weak) subsystem (B) remain disordered. Depending on the signs of  $J_b$  and  $J_{ab}$  exchanges and their ratio and on the geometry of the intersubsystem bonds, the further temperature decrease and the appearance of spontaneous magnetization in the subsystem B can

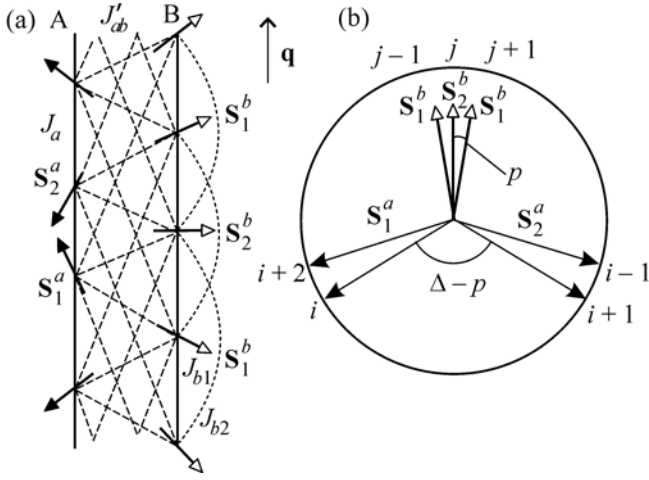


**Fig. 1.** (a) Distribution of spins and exchange interactions. (b) Relative local orientation of spins in the triangular incommensurate magnetic structure.

lead to topologically different noncollinear magnetic structures. The antiferromagnetic exchange ( $J_b > 0$ ) leads to the incommensurate magnetic structure with the locally orthogonal antiferromagnetism vectors of subsystems [12, 13]. The ferromagnetic exchange ( $J_b < 0$ ) stabilizes the Yafet–Kittel triangular ferromagnetic state [7]. The presence of antiferromagnetic exchange ( $J_{b2}$ ) with the next-nearest neighbors, which competes with the ferromagnetic exchange with the nearest neighbors ( $J_{b1}$ ) in the subsystem B, leads to the decrease in the energy of the B spins for magnetic structures with  $q > 0$ . The difference between the effective fields acting on the spins of different subsystems is responsible for different temperature dependences of the magnetizations of the subsystems and, as a consequence, for a temperature-induced change in the relative contributions of the subsystems to the general state. This can lead to a temperature-induced phase transition between the high-temperature collinear long-range order and the incommensurate magnetic structure or triangular Yafet–Kittel state at low temperatures, when the role of the magnetically weak subsystem increases. This work is aimed at studying the incommensurate states of a two-subsystem planar magnet with the geometrically frustrated intersubsystem exchange and the competition of exchanges between the nearest and next-nearest neighbors inside the second subsystem within the mean field approximation:

$$J_a > |J_{b1}| \geq J_{b2} \geq J_{ab}. \quad (1)$$

The length of the intersubsystem exchange bonds plays an important role in the formation of the incommensurate magnetic structure. A criterion of the selection of the orientation of the vector of the incommensurate magnetic structure along the direction of the largest length of frustrated bonds was proposed earlier [13].

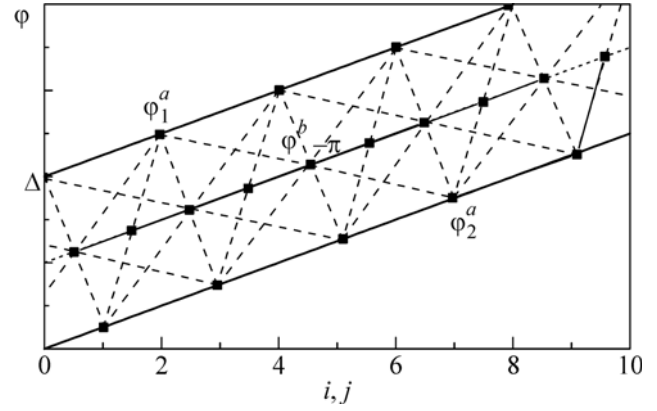


**Fig. 2.** Change in the angles of the spin orientation in the direction of the helix vector for a discrete magnet. Dotted lines show the intersubsystem exchange for models with  $l = 1$  and 3.

To estimate the effect of this factor, two models with the same relative exchanges but with different lengths of these bonds were considered:

$$\Delta c = (2l - 1)c/2, \quad l = 1, 3, \quad (2)$$

where  $c$  is the displacement between the ions of each subsystem along the vector of the incommensurate magnetic structure. The Hamiltonian of the model is

$$H = J_a \sum_{ii'} S_i S_{i'} + J_{b1} \sum_{jj'} S_j S_{j'} + J_{b2} \sum_{jj''} S_j S_{j''} + J_{ab}^l \sum_{ij} S_i S_j, \quad i \in A, \quad j \in B. \quad (3)$$

Only the main isotropic exchanges between spins  $S = 1/2$  in both subsystems are considered. The scheme of the spatial spin distribution and the geometry of the exchange interaction along the direction of the incommensurability vector  $\mathbf{q}$  and the local relative orientation of spins are shown in Figs. 1a and 1b, respectively. The spatial variation of the angles of the spin orientation of the antiferromagnetic sublattices of the subsystem A ( $\phi_{1,2}^a$ ) and subsystem B ( $\phi^b$ ) is shown in Fig. 2. For a discrete lattice, the canting angle between the neighboring spins of the subsystem A alternates as

$$\phi_1^a(i) - \phi_2^a(i \pm 1) = \Delta \pm p, \quad (4)$$

where  $\Delta$  is the canting angle between the antiferromagnetic sublattices of the subsystem A in the continuous approximation,

$$\Delta = \phi_1^a(x) - \phi_2^a(x),$$

and  $p$  is the pitch of the helix. Alternation leads to the different mean fields of the intersubsystem interaction on spins of the subsystem B and, consequently, to different mean values  $S_1^b$  and  $S_2^b$ . The subsystem B is sep-

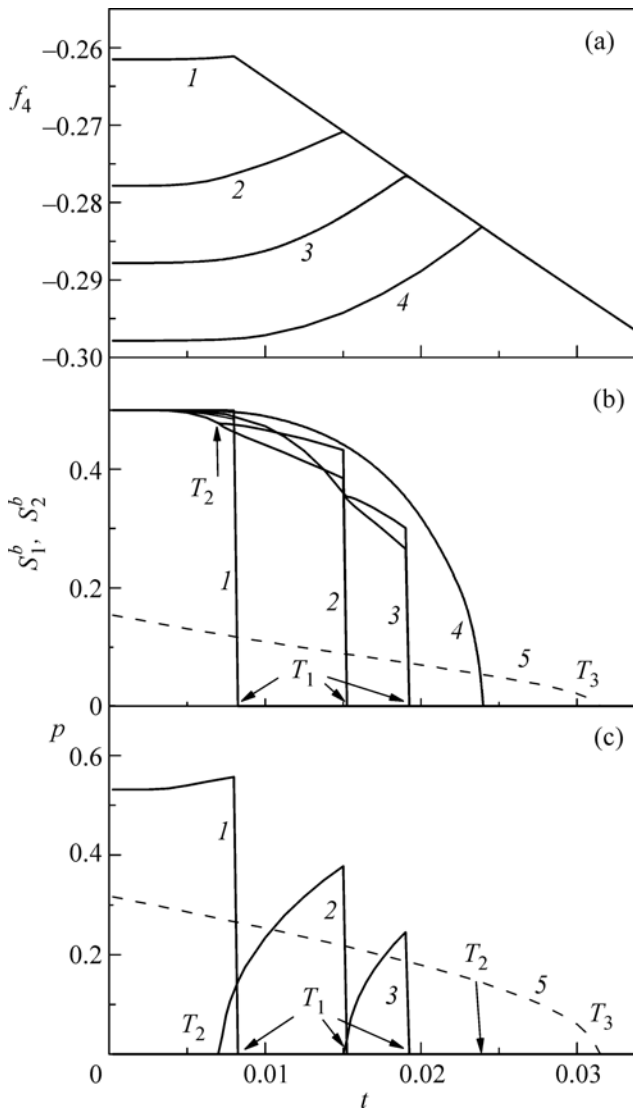


**Fig. 3.** Temperature dependences of (a) free energy, (b) mean values of spins in the subsystem B, and (c) pitch of helix. Lines 1–4 correspond to  $l = 1$  and the ratios between the competing exchanges in the subsystem B  $R = 1, 0.8, 0.7,$  and  $0.6,$  respectively, and lines 5 correspond to the mean values of B spins and pitch of the antiferromagnetic helix at  $l = 3$  and  $R = 0.6.$

arated into two ferrimagnetic sublattices. In contrast to amplitudes on the spins B, the amplitudes of the longitudinal mean fields on the spins A are the same:

$$h_l^a = h_{l1}^a = h_{l2}^a = \frac{z_a}{2} J_a S^a \cos \Delta \cos p$$

$$- \frac{z_{ab} J_{ab}^l}{4} \left[ (S_1^b + S_2^b) \cos \frac{\Delta}{2} \cos \frac{(2l-1)p}{2} \right.$$

$$\left. - (S_1^b - S_2^b) \sin \frac{\Delta}{2} \sin \frac{(2l-1)p}{2} \right],$$

$$h_{l1}^b = \frac{z_{b1}}{2} J_{b1} S_2^b \cos p + \frac{z_{b2}}{2} J_{b2} S_1^b \cos 2p \quad (5)$$

$$- \frac{z_{ba} J_{ab}^l}{2} S^a \cos \left[ \frac{\Delta}{2} + \frac{(2l-1)p}{2} \right],$$

$$h_{l2}^b = \frac{z_{b1}}{2} J_{b1} S_1^b \cos p + \frac{z_{b2}}{2} J_{b2} S_2^b \cos 2p$$

$$- \frac{z_{ba} J_{ab}^l}{2} S^a \cos \left[ \frac{\Delta}{2} - \frac{(2l-1)p}{2} \right],$$

where  $z_a, z_{b1}, z_{b2}, z_{ab},$  and  $z_{ba}$  are the numbers of neighbors for each of the spin–spin interactions. The relation  $z_{ab} = z_{ba}$  is assumed, although in the general case this relation can be different. At the equilibrium orientation of spins, the mean transverse fields on each spin are zero. For the spins A, this gives the equation

$$h_i^a = \frac{z_a}{2} J_a S^a \sin \Delta \cos p$$

$$- \frac{z_{ab} J_{ab}}{4} \left[ (S_1^b + S_2^b) \sin \frac{\Delta}{2} \cos \frac{(2l-1)p}{2} \right.$$

$$\left. + (S_1^b - S_2^b) \cos \frac{\Delta}{2} \sin \frac{(2l-1)p}{2} \right] = 0. \quad (6)$$

For the symmetric environment of the neighboring interacting spins, the transverse fields on spins B are always zero (Fig. 1b).

The free energy is additive in the mean field approximation. To find a configuration with its minimum value (the ground state), it is sufficient to minimize the energy of the minimum set of spins with the nonequivalent local environments. The numerical minimization of the free energy of four spins of this unit block is performed taking into account constraint (6) and self-consistency conditions imposed on the mean values of spins:

$$F_4 = -T(2 \ln Z^a + \ln Z_1^b + \ln Z_2^b), \quad (7)$$

$$Z_{1,2}^{a,b} = \text{Sp}(\exp H_{\text{MFA}}^{a,b}) = \exp\left(\frac{h_{1,2}^{a,b}}{2T}\right) + \exp\left(-\frac{h_{1,2}^{a,b}}{2T}\right), \quad (8)$$

$$S_{1,2}^{a,b} = -\frac{1}{2} \tanh\left(\frac{h_{1,2}^{a,b}}{2T}\right).$$

The dependences of the normalized free energy  $f_4 = F_4/z_a J_a$ , mean values  $S_{1,2}^b$ , and the pitch of helix  $p$  on the reduced temperature  $t = T/z_a J_a$  for the fixed values  $j_{b1} = z_{b1} J_{b1}/z_a J_a = -0.4, j_{ab} = z_{ab} J_{ab}^l/z_a J_a = 0.25$  and different relations between exchanges in the subsystem B ( $R = j_{b2}/|j_{b1}|, j_{b2} = z_{b2} J_{b2}/z_a J_a$ ) are shown in Fig. 3. For the given relations between exchanges of different subsystems, the mean value of spins in the subsystem

A  $S^a$  is close to saturation and hardly changes in the temperature interval under consideration. The appearance of the spontaneous magnetization in the subsystem B at  $T_1$  leads to the formation of a triangular incommensurate state when the threshold condition on the relation between the competing exchanges  $R > R_1$  is fulfilled. For the considered case,  $R_1 \approx 0.65$ . The magnetization in the subsystem B and the pitch of helix appear stepwise (a first-order phase transition occurs). The further temperature decrease reduces the pitch  $p$  (the wave vector of the incommensurate structure  $q$ ). At  $T_2$ , the magnet transfers to the Yafet–Kittel commensurate state if the ratio  $R$  is less than the second threshold value ( $R_2 \approx 0.9$ ) (lines 2 and 3 in Fig. 3). At  $R < R_1$ , the magnetization of the subsystem B arises after the second-order phase transition immediately forming the Yafet–Kittel commensurate phase (line 4 in Fig. 3). At  $R > R_2$ , there is no Yafet–Kittel phase and the triangular incommensurate magnetic structure remains the ground state down to zero temperature (line 1 in Fig. 3). In the incommensurate phase, the difference between the mean values of  $S_1^b$  and  $S_2^b$  spins is mainly determined by the intersubsystem exchange and temperature. At  $j_{ab} \ll 1$ , it is small (Fig. 3b).

The threshold conditions for the appearance of the incommensurate magnetic structure at  $T_1$  and its disappearance at  $T_2$  can be deduced analytically, taking into account that  $S_1^b = S_2^b = S^b$  at these points. The canting of the antiferromagnetic sublattices of the subsystem A and the simplified equation of the free energy minimization are obtained from Eqs. (6)–(8):

$$\cos \Delta / 2 = \frac{j_{ab} S^b \cos(2l-1)p/2}{2S^a \cos p}, \quad (9)$$

$$\frac{dF_4}{dp} = -2S^a \frac{dh_1^a}{dp} - 2S^a \frac{dh_1^b}{dp} = 0. \quad (10)$$

After algebraic transformations, the equation for the extremum  $p$  values is obtained in the form

$$\sin p \left\{ \frac{K(S^a)}{K(S^b)} - [j_{b1} + 4j_{b2} \cos p + j_{ab}^2 f_1(\cos p)] \right\} = 0, \quad (11)$$

$$K(S^{a,b}) = (S^{a,b})^2 \times \left[ 1 - \frac{1 - 4(S^{a,b})^2}{2S^{a,b}} \arctan(2S^{a,b}) \right]^{-1}, \quad (12)$$

$$f_1(\cos p) = \frac{1}{4 \cos^2 p},$$

$$f_3(\cos p) = \frac{1}{4 \cos^2 p} - 16 \cos^3 p + 10 \cos p.$$

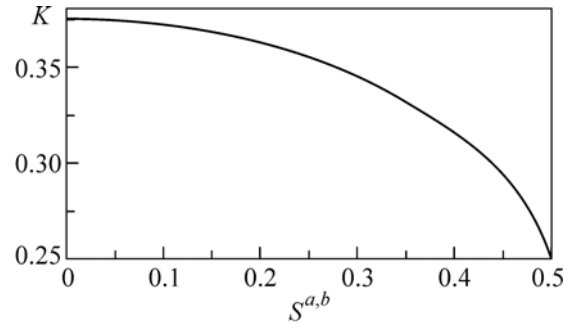


Fig. 4. Coefficients  $K(S^{a,b})$  versus the mean values of spins of the subsystems given by Eq. (12).

The first solution of Eq. (11),  $p = 0$ , corresponds to the homogeneous Yafet–Kittel triangular state. The second solution gives an equation for the pitch of the helix of the incommensurate state. Solutions with  $\cos p < 1$  appear if the threshold condition for the interactions is fulfilled. For  $l = 1$ , the threshold condition is

$$\frac{K(S^a)}{K(S^b)} < j_{b1} + 4j_{b2} + \frac{j_{ab}^2}{4}.$$

The main nontrivial result of this work is the temperature dependence of the pitch of the helix (wave vector of the incommensurate structure). The pitch of the helix of the incommensurate structure is maximal at the temperature of the appearance of the magnetization in the subsystem B  $T_1$  and then decreases. In spite of an increase in the contribution of the weak subsystem to the general state of the magnet, the wave vector decreases and the system tends to the formation of the Yafet–Kittel commensurate triangular structure. The coefficients  $K(S^{a,b})$  (Fig. 4) are determined by the temperature dependence of the magnetizations  $S^a$  and  $S^b$  (see Eq. (8)). For almost completely ordered subsystem A,  $K(S^a) \approx 1/4$  and the pitch of helix  $p$  depends only on  $K(S^b)$ . The limiting values of this coefficient,  $K(S^b \rightarrow 0) = 3/8$  and  $K(S^b \rightarrow 0.5) = 1/4$ , determine the interval of the exchange values for which there are the temperatures of appearance ( $T_1$ ) and disappearance ( $T_2$ ) of the incommensurate magnetic structure (Fig. 3, lines 2 and 3):

$$\frac{2}{3} < j_{b1} + 4j_{b2} + \frac{j_{ab}^2}{4} < 1. \quad (13)$$

When double inequality (13) is fulfilled, it can be stated that incommensurability appears via disorder, since during the complete ordering of the subsystem B ( $T = 0$ ), the states with  $q > 0$  are not ground ones. Outside this interval of interactions, either  $T_1$  or  $T_2$  is absent (Fig. 3, lines 4 and 1).

For the case of a more extended intersubsystem exchange along the vector of the incommensurate magnetic structure ( $l = 3$ ) when the threshold condition

$$R < R_3 \approx 0.77$$

is fulfilled, a long-periodic incommensurate magnetic structure with the locally antiferromagnetic sublattices in each subsystem—antiferromagnetic helix—appears between the Yafet–Kittel commensurate and antiferromagnetic phases simultaneously with the appearance of the magnetization in the subsystem B at the temperature  $T_3$ . After the appearance of the Yafet–Kittel triangular solutions at  $T_2$ , the system transfers to the Yafet–Kittel phase through the first-order phase transition. The pitch of the antiferromagnetic helix (wave vector) vanishes stepwise (Figs. 3b, 3c). The features of this structure arising in  $\text{CuB}_2\text{O}_4$  were considered earlier [12, 13]. In the intervals of the ratios of the competing interactions in the subsystem B

$$R_2 < R < R_3 < R_1$$

four phases with the phase transition sequence

Yafet–Kittel phase  $\longleftrightarrow$  triangular helix  
 $\longleftrightarrow$  antiferromagnetic helix  $\longleftrightarrow$  antiferromagnetic

are formed in a ferrimagnet at different temperatures.

Finally, some features of the triangular incommensurate structure and transitions limiting it are briefly discussed. This structure differs from the Kaplan ferrimagnetic helix in the mutual orientation of spins. The case under consideration is characterized by a Yafet–Kittel locally triangular orientation of four different sublattices (Fig. 1b) in contrast to the two-sublattice locally collinear ferrimagnetic orientation at the dominating intersubsystem exchange. Modulations of canting of the antiferromagnetic sublattices in the subsystem A and the mean values of spins in the subsystem B are due to the discreteness of the magnet. The additional unfrustrated subsystem leads to the enhancement of the classical threshold ratio for the appearance of the incommensurate magnetic structure,  $J_{b2}/|J_{b1}| > 1/4$  [9], although the frustrated intersubsystem exchange  $J_{ab}$  favors the formation of the incommensurate magnetic structure. When the threshold condition is fulfilled, the incommensurate magnetic structure appears with the finite pitch  $p > 0$  determined by Eq. (11). Consequently, the energy of the subsystem A increases by a finite value. Since the total energy of the system is continuous at the point of the phase transition (Fig. 3a), the energy of the subsystem B should decrease by the same finite value. This can occur only if the magnetization of the subsystem B appears at once with the finite nonzero value. Consequently, the first transition to the incommensurate state at  $T_1$  is a first-order phase transition. The situation with the second transition at  $T_2$  (the same as with the transition to the antiferromagnetic helix at  $T_3$ ) is not simple. Formally, it is a continuous transition between two topologically equivalent states and the magnetization in  $T_2$  has a kink characteristic of a second-order phase transition. At the same time, near  $T_2$  ( $\Delta t \sim 10^{-3}$ ), there is a macroscopic interval of solutions  $\Delta p \sim 10^{-1}$  with

almost the same values of energy ( $\Delta f_4 \sim 10^{-6}$ ). This means that, when the temperature decreases, the magnet transfers from the incommensurate phase to the Yafet–Kittel phase via the stochastic phase without a long-range order; i.e., there is general disordering as a result of an increase in the order (magnetization) in the subsystem B. The significant broadening of the stochastic layer between the periodic solutions in the phase space (in the vicinity of the separatrix) in comparison with the two-sublattice antiferromagnet at zero temperature is explained by an increase in the number of the dynamic variables in the two-subsystem (four-sublattice) magnet [14]. In addition, at a finite temperature, the number of degrees of freedom increases owing to the variation of the mean values of spins.

This work was supported by the Russian Foundation for Basic Research (project no. 10-02-00765).

## REFERENCES

1. A. P. Ramirez, *Ann. Rev. Mater. Sci.* **24**, 453 (1994); J. E. Greedan, *J. Mater. Chem.* **11**, 37 (2001); J. S. Gardner, M. J. P. Gingras, and J. E. Greedan, *Rev. Mod. Phys.* **82**, 53 (2010).
2. P. W. Anderson, *Phys. Rev.* **102**, 1008 (1956); J. Villain, *Z. Phys. B* **33**, 31 (1978).
3. J. N. Reimers, A. Berlinsky, and A.-C. Shi, *Phys. Rev. B* **43**, 865 (1991).
4. C. Pinettes, B. Canals, and C. Lacroix, *Phys. Rev. B* **66**, 024422 (2002).
5. N. P. Raju, M. Dion, M. J. P. Gingras, et al., *Phys. Rev. B* **59**, 14489 (1999); S. E. Palmer and J. T. Shalker, *Phys. Rev. B* **62**, 448 (2000).
6. M. Elhajal, B. Canals, R. Sanyer, et al., *Phys. Rev. B* **71**, 094420 (2005).
7. Y. Yafet and C. Kittel, *Phys. Rev.* **87**, 290 (1952).
8. T. A. Kaplan, *Phys. Rev.* **119**, 1460 (1960); D. H. Lyons, T. A. Kaplan, K. Dwight, et al., *Phys. Rev.* **126**, 540 (1962).
9. J. S. Smart, *Effective Field Theories of Magnetism* (Saunders, London, 1966; Mir, Moscow, 1968).
10. S. Martynov, G. Petrakovskii, and B. Roessli, *J. Magn. Magn. Mater.* **269**, 106 (2004).
11. M. Boehm, B. Roessli, J. Shefer, et al., *Physica B* **318**, 277 (2002); M. Boehm, B. Roessli, J. Shefer, et al., *Phys. Rev. B* **68**, 024405 (2003); Y. Kousaka et al., *J. Phys. Chem. Sol.* **68**, 2170 (2007); A. I. Pankrats, G. A. Petrakovskii, M. A. Popov, et al., *JETP Lett.* **269**, 569 (2004).
12. S. N. Martynov and A. D. Balaev, *JETP Lett.* **85**, 649 (2007).
13. S. N. Martynov, *J. Exp. Theor. Phys.* **108**, 72 (2009).
14. G. M. Zaslavskii and R. Z. Sagdeev, *Introduction to Nonlinear Physics* (Nauka, Moscow, 1988); S. N. Martynov and V. I. Tugarinov, *JETP Lett.* **92**, 115 (2010).

*Translated by L. Mosina*